THE JOURNAL OF PHYSICAL CHEMISTRY A

ARTICLE

pubs.acs.org/JPCA

Comprehensive NO-Dependent Study of the Products of the Oxidation of Atmospherically Relevant Aromatic Compounds

Adam W. Birdsall and Matthew J. Elrod*

Department of Chemistry and Biochemistry, Oberlin College, Oberlin, Ohio, 44074

Supporting Information

ABSTRACT: A comprehensive product study, performed via the turbulent flow chemical ionization mass spectrometry (TF-CIMS) technique, of the primary OH-initiated oxidation of many of the atmospherically abundant aromatic compounds was performed. The bicyclic peroxy radical intermediate, a key proposed intermediate species in the Master Chemical Mechanism (MCM) for the atmospheric oxidation of aromatics, was detected in all cases, as were stable bicyclic species. The NO product yield dependences suggest a potential role for bicyclic peroxy radical + HO_2 reactions at high HO_2/NO ratios, which are postulated to be a possible source of the inconsistencies between previous environmental chamber results and predictions from the MCM for ozone production and OH reactivity. The TF-CIMS product yield results are also compared to previous environment chamber results and to the latest MCM parametrization.

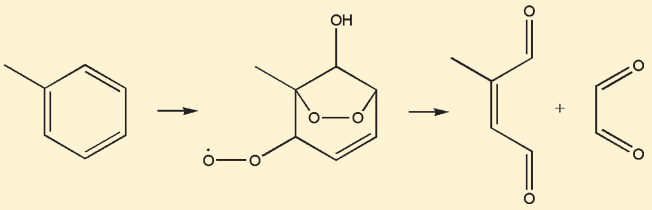

INTRODUCTION

Aromatic compounds play a key role in urban air pollution events. These largely anthropogenic compounds can comprise as much as 40% of the total nonmethane hydrocarbon (NMHC) content of the atmosphere in urban areas[1] and are known to efficiently lead to the formation of both tropospheric ozone and secondary organic aerosol (SOA) pollution.[2,3] The most atmospherically abundant aromatic species are typically benzene, toluene, dimethylbenzenes (xylenes), ethylbenzene, and trimethylbenzenes, which mainly arise from automobile exhaust, petroleum refining processes, and industrial solvent evaporation. The dominant atmospheric fate of these species is reaction with the OH radical, primarily by addition to the aromatic ring, but also by hydrogen atom abstraction at the alkyl groups.

The Master Chemical Mechanism (MCM) has been developed to provide an explicit representation of the initial OH reaction step for aromatics, as well as all subsequent reactions believed to play a role in the ultimate effect of aromatic oxidation chemistry on air quality.[4] The MCM primary OH-initiated oxidation mechanism for toluene is shown schematically in Figure 1. While the MCM was largely constructed from experimental observations of the organic reaction products of aromatic oxidation, one very important measure of the accuracy of the MCM concerns its ability to predict ozone production rates, as well as OH radical regeneration, under atmospheric conditions. Unfortunately, the MCM overpredicts ozone concentrations by 55% and underpredicts OH production by 44% in environmental chamber experiments meant to closely simulate atmospheric conditions for toluene oxidation.[4,5] Therefore, further refinements to the MCM are required to increase its efficacy in the overall effort to understand and reduce air quality problems related to elevated levels of aromatic compounds in the atmosphere.

In previous work, we investigated the products of the primary OH-initiated oxidation of toluene using the turbulent flow chemical ionization mass spectrometry (TF-CIMS) technique under different oxygen, NO, and initial OH radical concentrations as well as a range of total pressures.[6] The bicyclic peroxy radical intermediate, a key proposed intermediate species in the MCM for the atmospheric oxidation of toluene, was detected for the first time. The toluene oxidation mechanism was shown to have a strong oxygen concentration dependence, presumably due to the central role of the bicyclic peroxy radical in determining the stable product distribution at atmospheric oxygen concentrations. Based on these results, we proposed an initial set of reactions that can explain three of the four MCM product channels (Figure 2), and a set of reactions that depend on the bicyclic peroxy intermediate and lead to the fourth set of MCM products (Figure 3). The results also suggested a potential role for bicyclic peroxy radical + HO_2 reactions at high HO_2/NO ratios. These reactions were postulated to help explain inconsistencies between environmental chamber results and predictions from the MCM in terms of ozone production and OH radical regeneration of the toluene oxidation system.

Recently, several new investigations have been reported that attempt to address whether there are other important chemical processes missing from the MCM for the broader set of all atmospherically abundant aromatic compounds. Using TF-CIMS methods, Noda et al. detailed the existence of a new dealkylation pathway in the OH-initiated oxidation of toluene and the xylenes.[7] Specifically, it was noted that demethylated (or

Received: January 31, 2011
Revised: March 22, 2011
Published: May 09, 2011

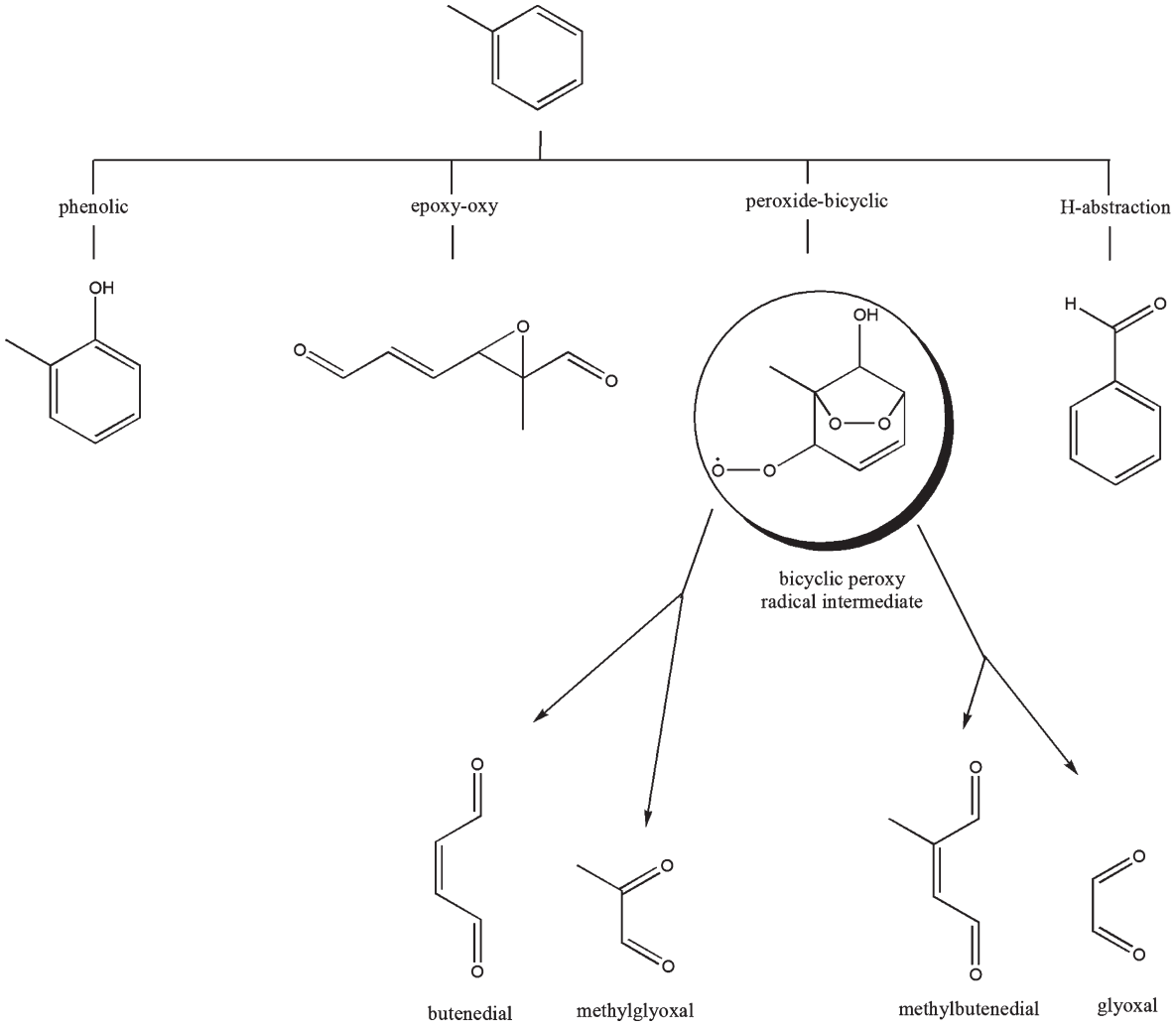

Figure 1. Master Chemical Mechanism (MCM) toluene oxidation mechanism (adapted from ref 4).

more generally, dealkylated) phenolic type compounds were formed in 5−10% yields for toluene and the xylenes. However, in an environmental chamber study of m-xylene and p-cymene, Aschmann et al. determined an upper limit of 1% for the dealkylation pathway.[8] Atkinson and co-workers also carried out photochemical environmental chamber experiments that explored the stoichiometric relationship between 1,2-dicarbonyl products (such as methylglyoxal in Figure 3) and unsaturated dicarbonyl products (such as butenedial in Figure 3) for a large number of aromatic precursors.[9,10] The mechanism given in Figure 3 (as does the MCM) predicts a 1:1 stoichoimetric relationship in the formation of these compounds. However, Atkinson and co-workers found that the unsaturated dicarbonyl products were often observed in significantly lower yields than the 1,2-dicarbonyls, their presumed product partners. Similar nonstoichiometric product yields have also been observed for benzene and toluene at the EUPHORE environmental chamber.[11]

Extending our previous study of the toluene oxidation system,[6] this article describes the identification of primary oxidation system intermediates and the detection and quantification of stable primary oxidation products for a variety of the most atmospheric abundant aromatic compounds via the turbulent flow chemical ionization mass spectrometry (TF-CIMS) technique. In particular, the CIMS approach allowed for a more complete identification of the reaction system species, and the TF method provided the facility to separately control OH, NO, and O_2 levels in the system, as well as to address the possible effects of heterogeneous or photochemical processes in previous environmental chamber experiments.

EXPERIMENTAL SECTION

Turbulent Fast Flow Tube. A schematic of the experimental apparatus is given in Figure 4 and is virtually identical to the method used in earlier work on toluene.[6] The main flow tube was 100 cm in length and constructed with 2.2 cm inner diameter Pyrex tubing. A large flow of variable amounts of oxygen and nitrogen carrier gas (30 STP L min^{-1}) was introduced at the rear of the flow tube to ensure turbulent flow conditions (Reynolds Number ≈ 2100 for most experiments). The reactants necessary for the production of OH radicals were prepared in a 20 cm long, 1.25 cm inner diameter side arm, while the aromatic compounds and NO were added to the rear of the flow tube, as shown in Figure 4. This arrangement allowed for the separate synthesis of OH radicals, but allowed all other reactants to be present simultaneously at the rear of the flow tube. For experiments involving the OH radical scavengers, the scavenger species were

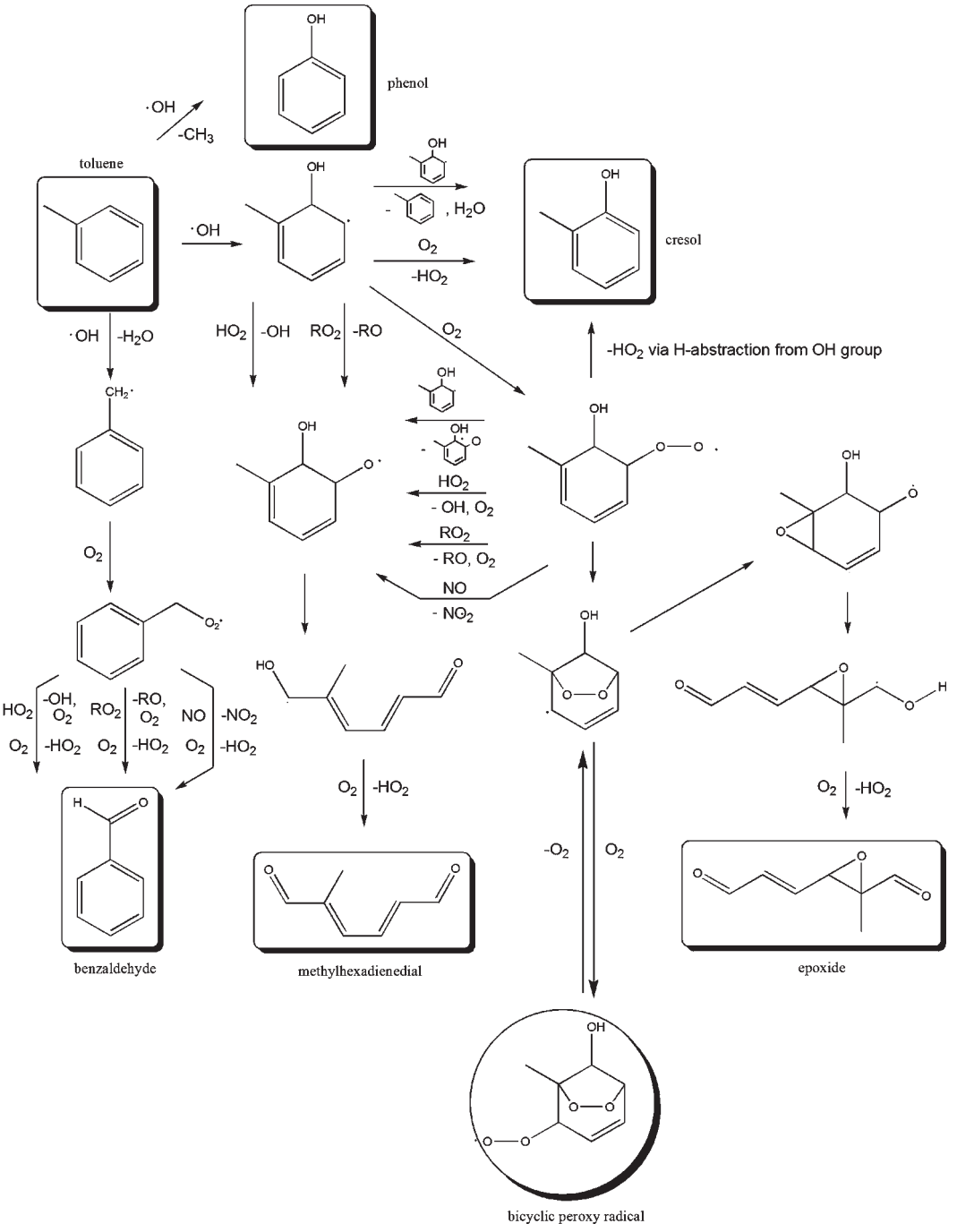

Figure 2. Nonbicyclic peroxy radical-dependent pathways in the primary OH-initiated oxidation of toluene.

introduced into the main flow tube through an encased moveable injector. The encasement was made of corrugated Teflon tubing and allowed the injector to be moved to various injector positions ("time = zero" injector position is set just upstream of the ionization source) without breaking any vacuum seals. A fan-shaped Teflon device was placed at the end of the injector to enhance turbulent mixing. All gas flows were monitored with calibrated mass flow meters. A polonium-210 (^{210}Po) α-particle-emitting ionization source was placed between the flow tube and the entrance to the CIMS. Flow tube pressure and temperature were measured upstream of the ionization source. Pressure was measured using a 0−1000 Torr capacitance manometer and maintained at 200 ± 2 Torr for all experiments. Temperature was determined using Cu-constantan thermocouples and was in the range 296−298 K for all experiments. Most of the flow tube gases were removed at the CIMS inlet using a 31 L s^{-1} roughing pump.

OH Source. The H + O_3 source utilizes the microwave discharge-initiated dissociation of H_2, followed by reaction with O_3:

$$H_2 \rightarrow H + H \quad (1)$$

$$H + O_3 \rightarrow OH + O_2 \quad (2)$$

A dilute mixture of He/H_2 was passed through a microwave discharge, produced by a Beenakker cavity operating at 50W, to

dx.doi.org/10.1021/jp2010327 |J. Phys. Chem. A 2011, 115, 5397–5407

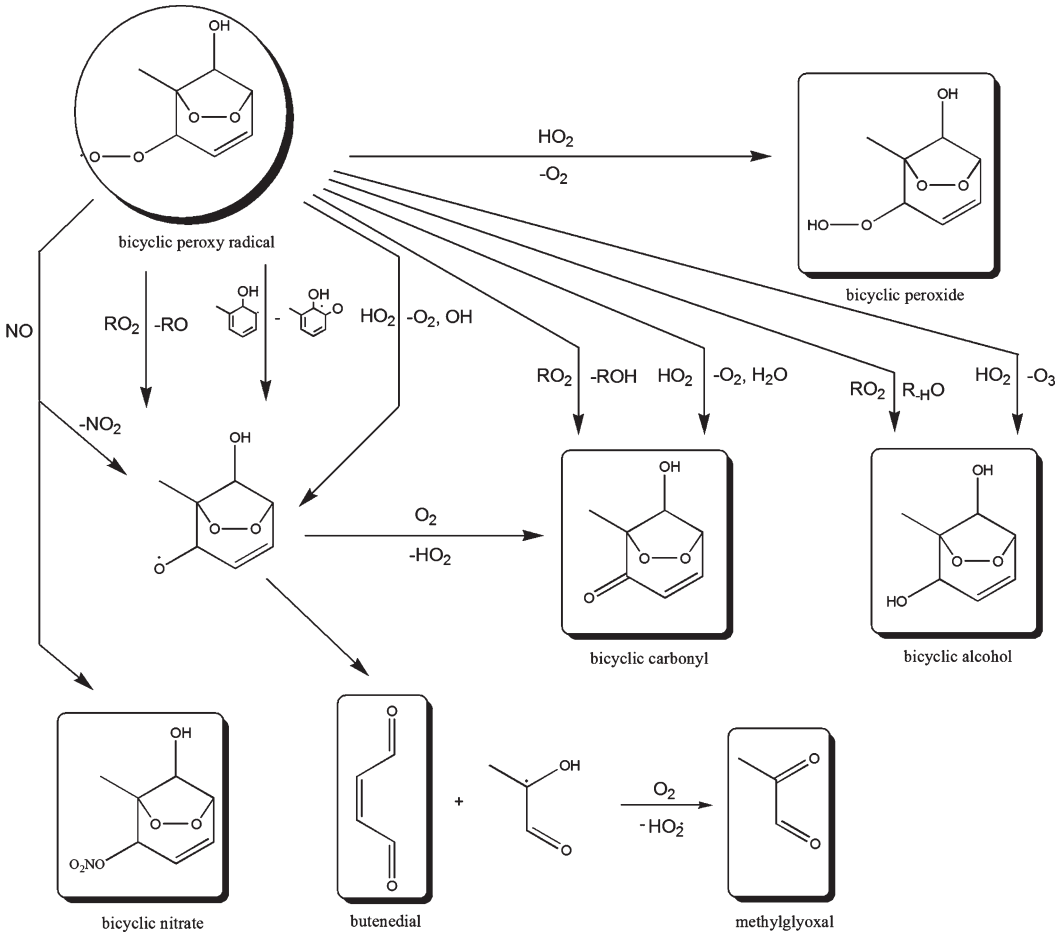

Figure 3. Bicyclic peroxy radical-dependent pathways in the primary OH-initiated oxidation of toluene.

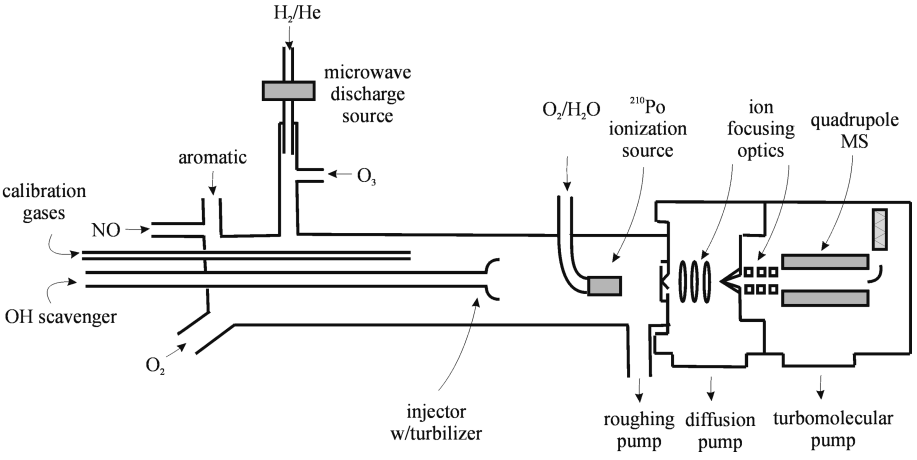

Figure 4. Experimental apparatus.

create hydrogen atoms (reaction 1). The dilute mixture was obtained by combining a 5.0 STP L min^{-1} flow of ultrahigh purity helium (99.999%) with a 1.0 STP mL min^{-1} flow of a 0.1−1.0% H_2 (99.9%)/He mixture. The 5.0 STP L min^{-1} helium flow was first passed through a silica gel trap immersed in liquid nitrogen to remove any possible impurities. The hydrogen atoms were then injected into the flow tube side arm and mixed with a flow of O_3 entrained in He. Ozone was produced in a commercial ozonizer and stored on a silica gel filled trap at −78 C. O_3 was introduced into the system by passing a 1−4 STP mL min^{-1} flow of He through the trap. Ozone partial pressures were determined by UV absorbance at 254 nm in a 1 cm flow-through quartz cuvette. Because O_3 was in great excess in the side arm ($[O_3] = \sim 2 \times 10^{13}$ molecules cm^{-3}) and the H + O_3 reaction is very fast (2.9×10^{-11} cm^{-3} $molecule^{-1}$ s^{-2}),[12] the OH-producing reaction has a very short lifetime of about 2 ms, thus, ensuring that all hydrogen

dx.doi.org/10.1021/jp2010327 |J. Phys. Chem. A 2011, 115, 5397–5407

atoms were quickly consumed (the minimum side arm residence time for OH is about 20 ms). The $OH + O_3 \rightarrow HO_2 + O_2$ reaction (which has a lifetime of 680 ms at the typical O_3 concentrations)[12] is expected to be of negligible importance in the side arm.

Aromatic Species. The benzene, benzene-d_6, toluene, toluene-d_3, toluene-d_8, ethylbenzene, ethylbenzene-d_{10}, *o*-xylene, *o*-xylene-d_{10}, *m*-xylene, *p*-xylene, *p*-xylene-d_{10}, 1,2,3-trimethylbenzene (TMB), 1,2,4-TMB, and 1,3,5-TMB systems were investigated. The aromatic compounds were added to the rear of the flow tube as either gas mixtures (benzene and toluene) or by flowing He carrier gas through room temperature traps (ethylbenzenes, xylenes, and TMBs). The aromatic concentrations were chosen such that OH-aromatic lifetime[12] was about 15 ms, which is short compared to the 100 ms main flow tube residence time for the aromatic compounds. These conditions ensured that the dominant fate of OH was reaction with the aromatic compound (the primary oxidation process of interest).

O_2 Dependence Studies. For the benzene and benzene-d_{10} systems, oxygen concentrations were varied by adjusting the fraction of oxygen in the 30 STP L min^{-1} carrier gas flow. At a total pressure of 200 Torr and with the carrier gas flow comprised entirely of oxygen, the main flow tube oxygen concentration was nearly that of the atmosphere at 760 Torr ($[O_2] = 5 \times 10^{18}$ molecules cm^{-3}). Therefore, the O_2 dependence studies were carried out at 200 Torr total pressure so that O_2 concentrations as high as atmospheric levels could be accessed.

NO Dependence Studies. NO [$(0-4) \times 10^{12}$ molecules cm^{-3}] was introduced into the main flow tube as a 2% NO/N_2 mixture at the same injection point as the aromatic species.

OH Scavenger Studies. For experiments involving benzene, *trans*-2-butene, which is known to efficiently form peroxy radicals in the presence of OH and O_2,[13] was introduced to the main flow tube as a 10% *trans*-2-butene/N_2 mixture through the moveable injector. To ensure that the *trans*-2-butene species outcompeted benzene for OH under these conditions, the concentration of *trans*-2-butene was chosen such that the OH-*trans*-2-butene lifetime[12] was 10 times shorter than the OH-benzene lifetime.

CIMS Detection. The chemical ionization reagent ions were produced using a commercial polonium-210 α-particle emitting ionization source consisting of a hollow cylindrical (69 by 12.7 mm) aluminum body with 10 mCi (3.7×10^8 disintegrations s^{-1}) of polonium-210 coated on the interior walls. All oxygenated organic species were detected using a proton transfer CIMS scheme. The $H^+(H_2O)_n$ ions were produced by passing a large O_2 flow (7 STP L min^{-1}) through the ionization source with H_2O impurities being sufficiently abundant to produce an adequate amount of reagent ions. The predominant species detected were the protonated (and partially hydrated) analogs of the neutral precursor oxygenated organic compounds. No fragment ions were detected. OH and HO_2 were detected via SF_6^- chemical ionization reactions, with OH^- and $SF_4O_2^-$ as the detected ions for each species, respectively.[14] SF_6^- reagent ions were produced by combining a large flow of N_2 (7 STP L min^{-1}) with a 1 STP mL min^{-1} flow of 10% SF_6/N_2 and passing the mixture through the ionization source. Ions were detected with a quadrupole mass spectrometer housed in a two-stage differentially pumped vacuum chamber. Flow tube gases (neutrals and ions) were drawn into the front chamber through a charged 0.1 mm aperture. The front chamber was pumped by a 6 in. 2400 L s^{-1} diffusion pump. The ions were focused by three lenses constructed from 3.8 cm inner diameter and 4.8 cm outer diameter aluminum gaskets and then entered the rear chamber through a skimmer cone with a charged 1.0 mm orifice. The skimmer cone was placed approximately 5 cm from the front aperture. The rear chamber was pumped by a 250 L s^{-1} turbomolecular pump. After the ions had passed through the skimmer cone, they were mass filtered and detected with a quadrupole mass spectrometer.

Relative Product Yield Studies. The relative product yield is defined as the flow tube concentration of the species of interest divided by the sum of the flow tube concentrations of all measured products. Therefore, the relative yield % is defined as follows:

$$\text{relative yield\%product } i = \frac{[\text{product } i]}{\sum_j^n [\text{product } j]} \times 100 \qquad (3)$$

This calculation requires the absolute concentrations of each product. Calibration curves for authentic samples of the products benzaldehyde and *o*-cresol were constructed by flowing a known concentration of each substance into the flow tube, and measuring the CIMS response. As extensively discussed in our earlier study on the toluene oxidation system,[15] because all other major products of the aromatic oxidation systems have either hydroxyl or carbonyl groups as the targets of the proton transfer CIMS reactions, it is reasonable to use the o-cresol or benzaldehyde (or the more convenient octanal) CIMS response factors, respectively, as proxy CIMS response factors for the calibration of species for which authentic samples are not available. All m/z charge carriers with signals with signal:noise ratios of greater than 2:1 were quantified (whether they could be definitively linked to a specific aromatic product species or not) so that the denominator in eq 3 could be determined as accurately as possible.

Total Aromatic Reactivity. The total amount of aromatic compound undergoing reaction can be determined by measuring the difference in aromatic concentration at the end of the flow tube with the OH source on and off. Since flow conditions alone determine the aromatic precursor concentration when OH is absent, the amount of reacted aromatic precursor is simply calculated from the ratio of the aromatic CIMS signal for the OH source on and off conditions, and the aromatic concentration when the OH source is off:

$$[\text{aromatic}]_{\text{reacted}} = \left[1 - \frac{(\text{aromatic CIMS signal})_{\text{OH source on}}}{(\text{aromatic CIMS signal})_{\text{OH source off}}}\right] \times [\text{aromatic}]_{\text{OH source off}} \qquad (4)$$

As we noted in our earlier work on toluene, the CIMS proton transfer method is not a very sensitive method for the detection of toluene, and we relied on an isobutane CIMS procedure for the in situ quantification of toluene.[6] However, this method was also hampered by the relatively small fraction of toluene that had reacted, making it difficult to accurately measure the difference in the two CIMS signals. In the present work, due to the reasonable CIMS proton transfer method sensitivity for the TMB systems and the significantly larger fraction of TMB that reacts (due to its larger OH rate constant), it was possible to more accurately determine $[\text{aromatic}]_{\text{reacted}}$ for the TMB systems and compare this quantity to the denominator in eq 3 to determine what fraction of the aromatic oxidation products have been quantified.

RESULTS AND DISCUSSION

Identification of Aromatic Oxidation Products. We were able to identify species belonging to most of the classes of the stable oxidation products indicated in Figures 2 and 3 (highlighted by boxes) for each of the aromatic species. However, in some cases, m/z coincidence issues, which were primarily caused by the presence of hydrates of the protonated product species, prevented the definitive identification and yield determination for some species: (1) The availability of totally deuterated isotopes determined whether we were able to separately measure the yields of the alkyl carbonyl (benzaldehyde for toluene specifically) and dienedial (methylhexadienedial for toluene specifically) products, as the protonated alkyl carbonyl and protonated dienedial monohydrate ions are m/z coincident for the normal isotopes, but have unique m/z ratios for the totally deuterated isotopes. For this reason, lumped alkyl carbonyl/dienedial yields are reported for the species for which only normal isotopes were available (o-xylene and all TMBs). (2) The availability of totally deuterated isotopes also determined whether we were able to separately measure the yields of the dealkylation product (phenol for toluene specifically) as the protonated dealkylation and the protonated alkyl glyoxal (methyl glyoxal for toluene specifically) monohydrate ions are m/z coincident for the normal isotopes but have unique m/z ratios for the totally deuterated isotopes. However, the protonated dealkylation product ion was also mass coincident with the protonated aromatic ion for the totally deuterated xylene species. Therefore, dealkylation product yields are reported only for toluene and ethylbenzene. (3) As we reported in our earlier toluene product study, the definitive identification of glyoxal and methylglyoxal was stymied for most of the aromatic systems by several m/z coincidences, some of which were also reported by Zhao et al.,[16] who used similar CIMS detection techniques. However, all presumed product partners for these species (such as methylbutenedial and butenedial respectively, for toluene) were definitively identified and quantified for all aromatic species. (4) In normal isotope experiments, the protonated bicyclic peroxy radical ions are detected at unique m/z ratios, but the protonated bicyclic peroxide and protonated bicyclic carbonyl monohydrate ions have m/z coincidences. However, for the totally deuterated aromatic species, the protonated bicyclic peroxide ions are detected at a unique m/z, while the protonated bicyclic peroxy radical ion and the protonated bicyclic carbonyl monohydrates are m/z coincident. Therefore, for the species for which totally deuterated isotopes were available, the bicyclic peroxy radical and bicyclic peroxide product could be uniquely measured, and the bicyclic carbonyl species yield could be determined by difference. However, for the other species, only a total "bicyclic" yield could be determined. (5) Because of m/z coincidence issues for the protonated epoxide monohydrate and protonated bicyclic alcohol ions, we could not definitively confirm the presence of the bicyclic alcohol species previously observed in the 1,3,5-TMB experiments of Wyche et al.[17] However, because the signal for bare protonated epoxide ion (which has no m/z coincidences with other predicted species) was generally much larger than the signal at the m/z coincident value for the epoxide and the bicyclic alcohol species, we are confident that the epoxide species has been definitely identified and that the yield is reasonably accurate.

Oxygen Dependence of Relative Product Yield for Benzene. In our previous studies of the toluene oxidation system,[6,15] we found that at low O_2 concentrations, the stable species shown in Figure 2 are dominant, but at higher O_2 concentrations, the species shown in Figure 3 become much more important.[6] Figure 5 shows the O_2 dependence of the product yields for benzene obtained in the present work. Similar to what was found the O_2 dependence of the observed products from toluene, the O_2 dependence plateaus between 1 and 2 $\times$ 10^{18} molecules cm^{-3}, just short of the ground level atmospheric value of 5 $\times$ 10^{18} molecules cm^{-3}. Again, we conclude that the overall O_2 dependence is explained by the rising concentration (and reactivity) of the bicyclic peroxy radical intermediates as O_2 levels are increased.

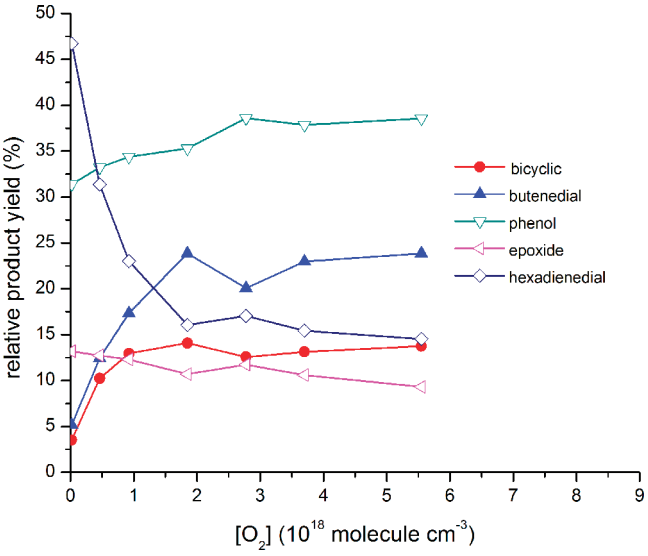

Figure 5. NO-free oxygen concentration dependence of benzene oxidation product yields.

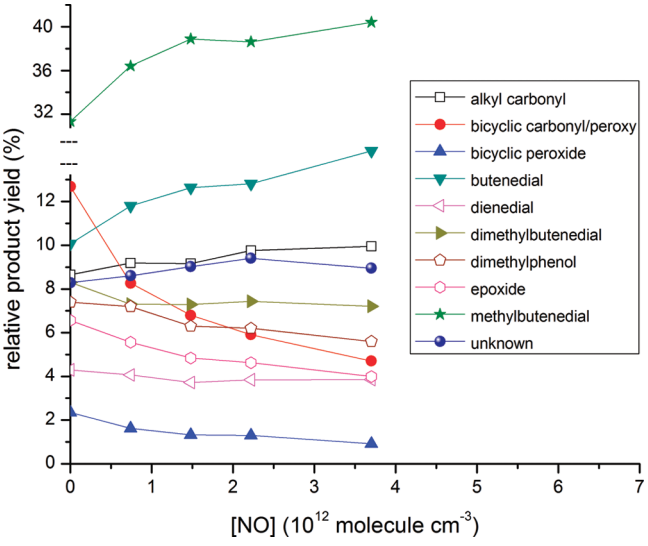

Figure 6. NO concentration dependence of *o*-xylene oxidation product yields.

Evidence for OH Regeneration. As in our previous work on the toluene oxidation system,[6] SF_6^- CIMS methods revealed that our OH source also produces some HO_2. HO_2 is likely produced via the H + O_2 reaction in the side arm, with O_2 arising from the decomposition of O_3 in the silica gel trap and in the tubing from the trap to the side arm. When 1,3,5-TMB was added to the system under NO_x-free conditions, HO_2 levels were observed to increase. Under the same 1,3,5-TMB conditions, OH levels were observed to

dx.doi.org/10.1021/jp2010327 |J. Phys. Chem. A 2011, 115, 5397–5407

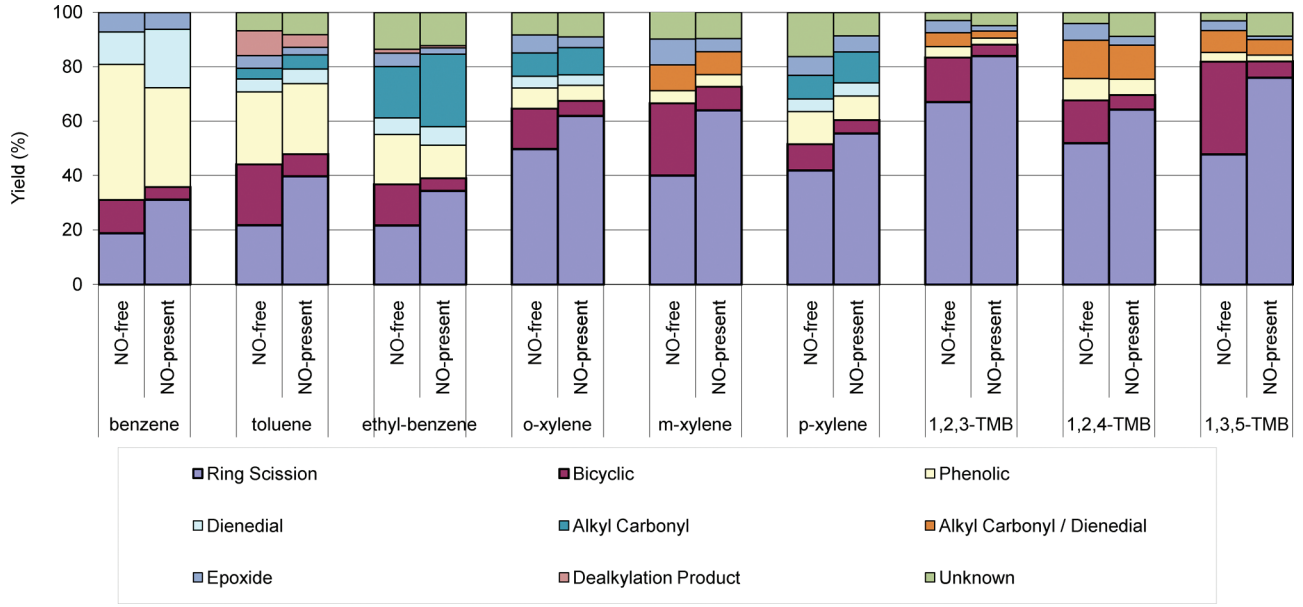

Figure 7. Summary of aromatic oxidation product yields.

decrease, but not to background levels, as would be expected given the short lifetime of the OH + 1,3,5-TMB reaction compared to its residence time in the flow tube. Considering the persistence of OH under these conditions, it is clear that the 1,3,5-TMB oxidation system regenerates OH.

To further probe the OH-regenerating nature of the aromatic oxidation system, scavenger experiments for benzene were carried out under NO_x-free conditions at an O_2 concentration of 5×10^{18} molecules cm^{-3}, with the *trans*-2-butene scavenger added at a position downstream of the benzene injection point (50 ms) such that the initial OH + benzene reaction (lifetime = 15 ms) has had more than 3 lifetimes to react (>95% reaction completion). Under the conditions used, the lifetime of OH with respect to *trans*-2-butene was only 2 ms; therefore, OH was virtually instantaneously converted to the *trans*-2-butene hydroxy peroxy radical. When the CIMS response factor is used for a similar hydroxy species (cresol), the absolute concentrations of the *trans*-2-butene hydroxy peroxy radical were determined. Similar to what was observed in our previous study of toluene,[6] a significant OH production rate was observed in the NO_x-free benzene oxidation system (1.2 ± 0.2 (2σ) $\times 10^{11}$ molecules cm^{-3} s^{-1}). Therefore, although we have only spot-checked for OH regeneration using direct OH detection and trans-2-butene scavenging methods for the benzene, toluene, and 1,3,5-TMB systems, it is reasonable to conclude that OH regeneration is a general feature of the NO_x-free aromatic oxidation mechanism.

NO Dependence of Relative Product Yields. Figure 6 shows the relative product yield results for the *o*-xylene-d_{10} NO dependence experiments at an O_2 concentration of 5×10^{18} molecules cm^{-3}. Typical total identified product concentrations were about 2×10^{11} molecules cm^{-3}. The main sources of error in the product yield measurements were run-to-run variability (~20%, presumably due to slightly different flow tube conditions) and CIMS response factor variability (~20%).

As we had determined earlier for toluene,[6] increased NO concentrations favor the formation of the ring scission species, while the ring-retaining bicyclic species are suppressed by high levels of NO. However, the species in Figure 2 (nonbicyclic peroxy radical-dependent) are little affected by NO, and all of the bicyclic peroxy radical pathway-dependent species are observed even in the complete absence of NO.

Figure 7 reports the relative product yield results for NO-free and NO-present ([NO] = 3.7×10^{12} molecules cm^{-3}) experiments for all systems under study. The tabulated relative product yield data is reported in Table S1 in the Supporting Information. As discussed above, the bicyclic species are lumped together for all aromatic species and the alkyl carbonyl and dienedial species are lumped together for the aromatics for which deuterated isotopes were not available. It is important to note that, under NO-free conditions, the bicyclic species are major products, with yields ranging from 10 to 30%. To make comparison across the different aromatic species more convenient, the ring scission products (such as butenedial and methylbutendial for toluene specifically) are also lumped together. The presentation in Figure 7 shows quite clearly that NO plays a role in the partitioning of the observed products between bicyclic and ring scission products. In other words, the sum of these two lumped categories is roughly the same for NO-free or NO-present experiments for each aromatic, but the presence of NO leads to a higher proportion of ring scission products. It's also clear that the proportion of total oxidation products in the summed bicyclic/ring scission categories increases as the extent of alkylation of the aromatic compound increases, while the phenolic proportion decreases proportionally. This is probably due to the increasing likelihood of more stable tertiary bicyclic radical intermediates in the more highly alkylated aromatics, which then leads to a greater proportion of these intermediates going on to form bicyclic peroxy radical intermediates. The dienedial and epoxide products are observed as minor species in all systems, and, with the exception of benzene, show no strong aromatic species- nor NO-dependence. For benzene, the dienedial yields are larger than for any other system, and are observed to increase significantly with NO, a result previously observed by Berndt and Boge, albeit at a significantly higher NO concentration than in the present work.[18] For the alkyl carbonyl products, it is clear that this pathway is much more important for ethylbenzene than for

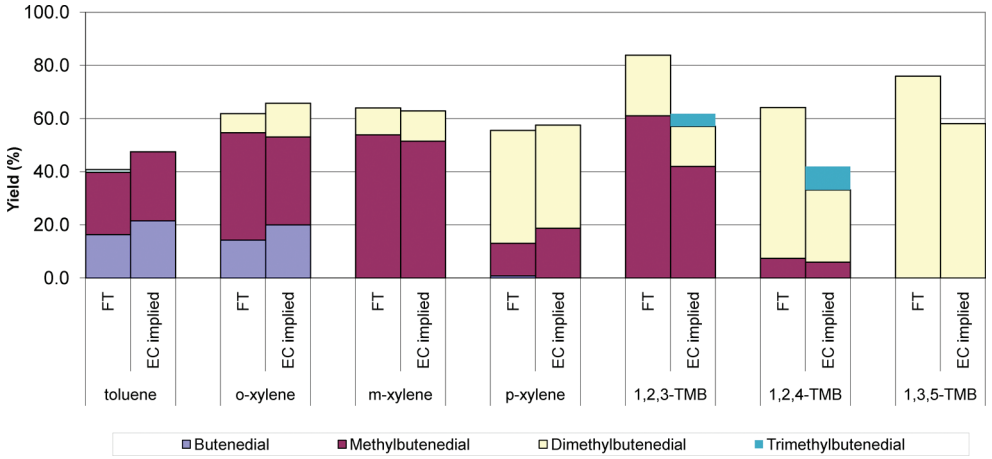

Figure 8. Comparison of present ring scission product yields (FT) to those stoichiometrically implied by previous environmental chamber (EC implied) results (ref 10).

the other alkylated aromatics, which is most likely due to the increased hydrogen abstraction pathway reactivity of the methylene group in ethylbenzene. We were also able to positively identify bicyclic nitrate products produced in the NO-present oxidation of the TMBs based on the observation of NO-dependent signals at the appropriate m/z values. However, as these products were observed at below 1% yield (assuming a CIMS response factor equal to that of *o*-cresol) and difficult to measure accurately, we do not report specific yield values for the bicyclic nitrate species.

Total Product Yields versus Total Aromatic Reactivity. To better establish the proportion of products identified and quantified in the present study, all significant m/z carriers were converted to an effective product concentration, as detailed in the Relative Product Yield Studies section of this paper. If the particular m/z carrier could not be assigned to a particular aromatic product, it was assigned to a category labeled "unknown." Figure 7 indicates that for every aromatic system, at least 80% of quantified products were assigned to a particular oxidation product identity. Further, to address whether a significant proportion of products of aromatic oxidation have eluded detection by our CIMS analytical approach, we also determined the total aromatic reactivity of the TMB oxidation systems (in the manner described above in the Experimental Section). The total quantified product yields made up 110, 82, and 95% of the observed aromatic reactivity for the 1,2,3-, 1,2,4-, and 1,3,5-TMB systems, respectively (with estimated errors of ±20% due to CIMS response factor variability). Therefore, a large majority of the aromatic oxidation products have apparently been quantified in our CIMS approach. Because it is difficult to envision unidentified aromatic oxidation products that do not contain at least one oxygen atom, and the proton transfer CIMS method is completely general for any oxygen containing organic compound (owing to the high proton affinity of oxygen atoms that are bonded to carbon atoms), this result is not surprising.

Insights on the Dealkylation Pathway. In their study of the dealkylation pathway in the OH-initiated oxidation of the normal isotopes of toluene, *o*-xylene, *m*-xylene, and *p*-xylene using a similar TF-CIMS approach, Noda et al. have reported dealkylation yields of 5.4, 11.2, 4.5, and 4.3%, respectively.[7] However, Aschmann et al., using an environmental chamber coupled with a GC-FID analytical approach, have recently reported a 1% upper limit dealkylation product yield for *m*-xylene.[8] Aschmann et al. further suggested that the isobaric oxepin species might be responsible for the m/z carriers observed in the Noda et al. experiments. As discussed above in the Identification of Aromatic Oxidation Products section, due to m/z coincidence issues, we were only able to determine dealkylation product yields for toluene and ethylbenzene, which were determined to be, in the presence of NO, 4.7 and 0.8%, respectively. While it is possible that the presence of an ethyl group significantly depresses the dealkylation pathway (perhaps by increased resonance stabilization of the radical intermediates proposed by Noda et al.) and explains our quite different dealkylation yields, it remains unclear whether the dealkylation pathway is a significant oxidation pathway for aromatic compounds.

Insights on the Ring Scission Pathway. It has long been assumed that the ring scission pathway leads to two products in which the total number of carbon atoms present in the original aromatic compound is conserved in the two ring scission products (such as is shown in Figure 3 for 7-carbon toluene: ring scission leads to identical yields of either the 4-carbon butenedial/3-carbon methylglyoxal product pair or to identical yields of the 5-carbon methylbutenedial/2-carbon glyoxal product pair). However, it has been difficult to validate this carbon conservation rule in part due to analytical difficulties, as well as questions concerning possible secondary chemistry of these species under certain experimental conditions. Arey et al. recently reported the results of environmental chamber experiments for a variety of aromatic compounds, using derivatization GC−CIMS detection methods to selectively identify all possible ring scission products.[9] In some cases, the carbon conservation rule was shown to be valid. However, for other cases, the larger ring scission product was observed in lower yields than the smaller ring scission product (the 1,2-dicarbonyls such as glyoxal, methylglyoxal, and dimethylglyoxal (biacetyl)). In particular, Arey et al. reported that, with the exception of butenedial, the larger ring scission products with unsaturated aldehyde functionality were found at systematically lower yields than their corresponding 1,2-dicarbonyl smaller ring scission coproduct. This result suggested that either the product pair carbon conservation rule is not followed in certain ring scission pathways or that the unsaturated aldehyde ring scission products were further reacting (either photolytically or heterogeneously) in the environmental chamber experiments. While the present experiments could not directly address this issue

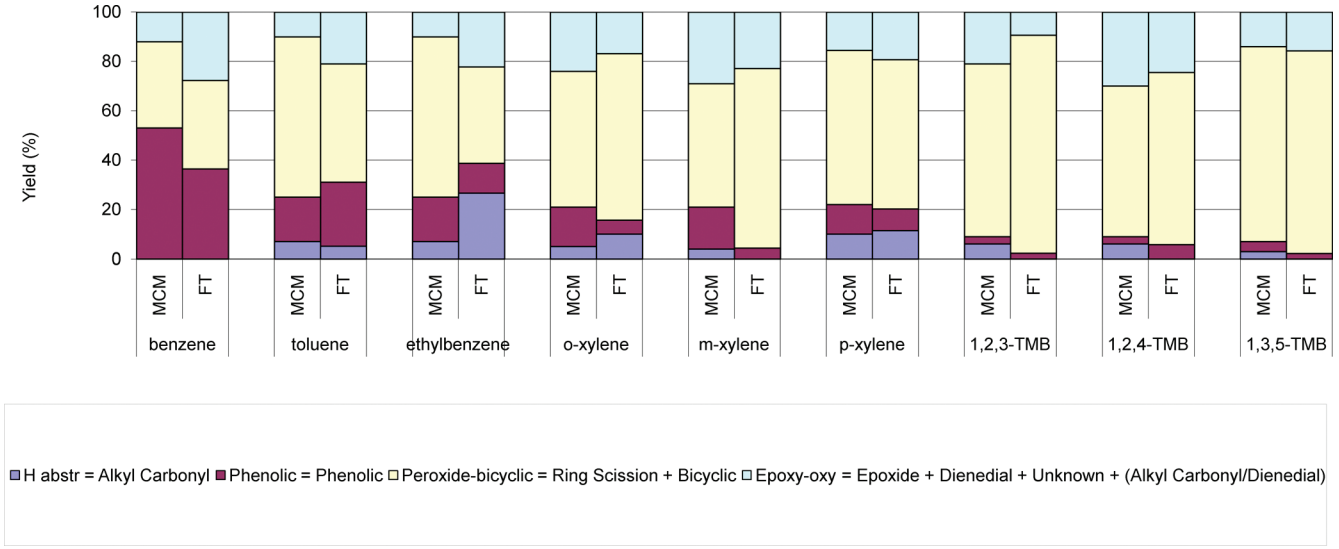

Figure 9. Comparison of present lumped product yields (FT) to those indicated by the Master Chemical Mechanism (MCM; ref 4).

(due to our inability to quantify glyoxal and methyglyoxal yields), our yields for the larger ring scission products were measured under wall-less,[19] nonphotolytic conditions. Therefore, a comparison between the present flow tube experiments and the environmental chamber experiments can provide some insight on the validity of the carbon conservation rule.

Because environmental chamber experiments are typically carried out at relatively high NO_2 concentrations, Nishino et al.[10] explicitly investigated the NO_2-dependence of the 1,2-dicarbonyl yields for the same set of aromatic compounds previously studied by Arey et al.[9] to be able to extrapolate the 1,2-dicarbonyl yields to zero NO_2 concentration. These values (with reported errors of between 0.7 and 8.5%) are expected to be more relevant for atmospheric conditions, as well as the conditions used in the present experiments. Therefore, we used the 1,2-dicarbonyl yields reported by Nishino et al. and the unsaturated dicarbonyl/1,2-dicarbonyl ratios reported by Arey et al. to derive a unified set of environmental chamber product yield values for all species. For example, Arey et al. reported that the measured methylglyoxal yield from 1,3,5-TMB was about six times more than its presumed coproduct, dimethylbutenedial, and Nishino et al. showed that the zero NO_2 methylglyoxal yield for 1,3,5-TMB was 58%. Applying the carbon conservation rule to the results of Nishino et al. suggests that the dimethylbutenedial yield for 1,3,5-TMB should be 58% in the absence of secondary chemistry. Because the measured environmental chamber dimethylbutenedial yield was only about 10%, the postulated influence of secondary chemistry in the environmental chamber experiments is quite large. In the present flow tube experiments, the measured yield for dimethylbutenedial from 1,3,5-TMB oxidation was determined to be 76%, a value consistent (within the stated errors of the present technique, ±20%) with the implied environmental chamber value of 58% but much larger than the actual measured environmental chamber value of 10%. Figure 8 reports the yields of the larger ring scission products (in the presence of NO) determined in the present flow tube experiments, as well as the implied environmental chamber larger ring scission product yields based on the carbon conservation rule for all aromatic systems. The data depicted in Figure 8 is reported in Table S2 in the Supporting Information.

Inspection of Figure 8 indicates that the present wall-less and dark measurements of the larger ring scission products for all of the aromatic compounds are consistent with the previous environmental chamber measurements of the smaller ring scission products, assuming the validity of the carbon conservation rule. Therefore, it appears that the violations of the carbon conservation rule observed by Arey et al. are likely due to secondary degradation of the larger unsaturated aldehyde ring scission products. Similar secondary degradation of the dienedial products identified in the present work might also explain why dienedial products (which are also unsaturated aldehydes) have been detected in other dark flow tube aromatic oxidation experiments[6,7,16,18] but are generally not observed in environmental chamber experiments.[9]

Implications for the Aromatic Oxidation Mechanism. In general, the present results for a larger set of the atmospherically abundant aromatic compounds are consistent with the conclusions drawn from our earlier work on the toluene oxidation system. In particular, the direct observation of the bicyclic peroxy radical intermediate and stable bicyclic products for all aromatic species in the present work serves to underline the importance of the bicyclic pathway in the oxidation of aromatic compounds. Therefore, we believe that Figures 2 and 3, which outline the specific oxidation mechanism for the ortho OH attack on toluene, can be used as a general guide for the oxidation mechanism for the other aromatic compounds.

Based on the large body of experimental work existing at the time of its latest revision, the Master Chemical Mechanism (MCM v3.1, 2005) provides the most explicit representation of individual chemical reactions that make up the overall aromatic oxidation process.[4] Product studies have been the most common input into the construction of the MCM, and the agreement between these studies and the MCM is one measure of the accuracy of the MCM itself. Therefore, it is of interest to compare the results of the present product study (in the presence of NO) to the product predictions of the MCM. As discussed in the Introduction and depicted in Figure 1, the MCM assumes four major product categories for the primary OH-initiated oxidation of aromatics: (1) phenolic, (2) epoxy-oxy, (3) peroxide-bicyclic, and (4) H-abstraction. However, as the epoxy-oxy

species has been observed in only a few studies, the epoxy-oxy category in the MCM is actually a "catch-all" category that is used to ensure carbon mass balance (i.e., that the total product yield adds up to 100%). To compare the present results to the MCM, the following correspondences were made, respectively: (1) phenolic = phenolic, (2) epoxide + dienedial + unknown = epoxy-oxy, (3) ring scission + bicyclic = peroxide bicyclic, and (4) alkyl carbonyl = H-abstraction. Therefore, the lumped epoxy-oxy categorization of the present results includes the actual quantified epoxide and dienedial yields, along with the "unknown" product yields. In addition, for the species for which no totally deuterated isotopes were available, the alkyl carbonyl yields could be not individually quantified. Therefore, there are no H-abstraction yields reported for the present results for *m*-xylene and the TMBs; rather, the H-abstraction yields for these species are actually represented in the catch-all epoxy-oxy category. These four categories were used to compare the present results and the MCM across all aromatic species in Figure 9. The data depicted in Figure 9 is reported in Table S3 in the Supporting Information. With a few exceptions, the present results are in good agreement with the MCM predictions. In particular, the MCM accurately predicts the greater importance of the bicyclic pathway for the more highly alkylated aromatics. However, the MCM greatly underpredicts the H-abstraction pathway for ethylbenzene (because it uses the toluene value as the basis for its prediction) and seems to somewhat overpredict the phenolic pathway for the xylenes.

Of course, the ultimate purpose of the MCM is to provide a model that can accurately predict the quantity of air pollutants, such as O_3 and SOA, produced by the oxidation of aromatic compounds under typical atmospheric conditions. Therefore, as discussed in the Introduction, the MCM has been tested against the results of environmental chamber experiments meant to closely simulate atmospheric conditions and has been found to overpredict O_3 production and to be missing processes that regenerate OH with little NO to NO_2 conversion.[4,5] In particular, the MCM predicts that the dominant fate of the toluene-derived bicyclic peroxy radical under atmospheric and the usual environmental chamber conditions is reaction with NO to form the bicyclic alkoxy radical that goes on to scission to form the butenedial (and methylglyoxal) and methylbutenedial (and glyoxal) products; this reaction also accomplishes the important NO to NO_2 conversion that is characteristic of mechanisms that contribute to tropospheric ozone production. As in our previous work on toluene[6] and in other NO-free experiments[20−22] reported in the literature, the present results suggest that significant bicyclic peroxy radical reactivity may exist in the absence of NO. Figure 3 depicts several other reactive pathways for the bicyclic peroxy radical that attempt to rationalize the observed products under NO_x-free conditions, as well as the observation of stable bicyclic species and OH regeneration. In our previous work on the toluene system, we proposed that peroxy−peroxy reactions are responsible for the observed reactivity of the bicyclic peroxy radicals under NO_x-free conditions. By analogy to the results obtained for the products formed from the self-reactions of alkene-derived peroxy radicals,[23]

$$RO_2 + R'O_2 \rightarrow RO + R'O + O_2 \quad (5)$$

$$\rightarrow ROH + R'_{-H}O + O_2 \quad (6)$$

$$\rightarrow R_{-H}O + R'OH + O_2 \quad (7)$$

and from the reactions of acetyl peroxy radicals with hydroperoxy radical:[24,25]

$$RO_2 + HO_2 \rightarrow ROOH + O_2 \quad (8)$$

$$\rightarrow ROH + O_3 \quad (9)$$

$$\rightarrow RO + OH + O_2 \quad (10)$$

Because some HO_2 is initially present as a byproduct of the OH source used in our experiments and HO_2 is produced by many of the individual reactions shown in Figures 2 and 3, HO_2 concentrations are likely to be higher than bicyclic peroxy radical concentrations under our experimental conditions (and this is certainly true of the atmosphere, as well). Further, $RO_2 + HO_2$ rate constants tend to be larger than $RO_2 + R'O_2$ rate constants (by factors of 20−1000 for secondary and tertiary peroxy radicals such as the bicyclic peroxy radical).[23] In our earlier work on toluene,[6] we found that the product yields did not depend on the initial radical dependence, as one might expect if $RO_2 + R'O_2$ reactions were responsible for some of the product species. Further, since most of the aromatic systems under study in the present work have more alkyl substitution than toluene, the $RO_2 + R'O_2$ reactions are likely to be, on average, even slower than they are for toluene. Thus, it appears that $RO_2 + HO_2$ reactions are more likely to be important in under our experimental conditions than are $RO_2 + R'O_2$ reactions. We note that the observation of the bicyclic peroxide product in our experiments directly indicates that at least some of the bicyclic peroxy radical reactivity is due to HO_2 reaction. Indeed, reactions 8 and 10 can account for all of the bicyclic peroxy radical reactivity and the resulting observed products under NO_x-free conditions and can explain the presence of OH regeneration for the toluene systems as follows: (1) the bicyclic peroxide product is produced directly via reaction 8 and (2) the butenedial (and methylbutenedial), bicyclic carbonyl, and OH products are formed via reaction 10. In our previous work on toluene, we used estimates of the radical concentrations to enable a kinetic analysis of the hypothesis above, and concluded that reaction 10 would likely have to be a major pathway to explain the observed OH regeneration rate and the presence of high yields of bicyclic and ring scission products under NO_x-free conditions. Because very similar behavior was observed in the present study, we refer to the reader to our previous work on toluene for the details of the approximate kinetic argument,[6] rather than repeat the analysis here. In any case, it would be highly desirable to experimentally determine the specific rate constants for the $RO_2 + HO_2$ and $RO_2 + NO$ reactions for the bicyclic peroxy radicals so that the above hypothesis can be rigorously tested.

CONCLUSION

In general, our results for the larger class of atmospherically abundant aromatic compounds are quite similar to our previous results for toluene. In particular, our experiments suggest that, at least at high HO_2 and low NO concentrations, $RO_2 + HO_2$ reactions involving the bicyclic peroxy radical can be competitive with the $RO_2 + NO$ reactions that facilitate NO to NO_2 conversion for all aromatic compounds. If the HO_2/NO ratios were high in the previous environmental chamber results used to test the MCM,[4] these reactions may have led to the overprediction of ozone by the MCM. Unfortunately, HO_2 concentrations were not directly measured in these experiments; therefore, this hypothesis must remain speculative. Further, because reaction 10

also produces OH, it can also explain the environmental chamber observation of significant OH regeneration.

Within the uncertainty limits of our product yield measurements, we determined that the yields of the unsaturated dicarbonyl compounds, formed through the bicyclic peroxy radical ring scission pathway, were in stoichiometric equivalence (i.e., obeyed the carbon conservation rule) with the 1,2-dicarbonyl yields measured in previous photochemical environmental chamber techniques.[9,10] Because many of these unsaturated dicarbonyl compounds were measured in lower yields in the environmental chamber measurements and our experiments were photochemically dark and wall-less, it seems likely that these species are undergoing secondary chemistry under the conditions of the environmental chamber experiments.

The overall product yields were in reasonable agreement with the predictions from the MCM. However, we measured a number of potentially important products not currently included in the MCM (dienedials and stable bicyclic species for all aromatic systems). Our results also suggest that the phenolic yields for the xylenes are too high and the H-abstraction yields for ethylbenzene are too low in the current version of the MCM.

■ ASSOCIATED CONTENT

Supporting Information. Three tables containing the data graphically depicted in Figures 7−9. This material is available free of charge via the Internet at http://pubs.acs.org.

■ AUTHOR INFORMATION

Corresponding Author
*E-mail: mjelrod@oberlin.edu.

■ ACKNOWLEDGMENT

This material is based upon work supported by the National Science Foundation under Grant No. 0753103.

■ REFERENCES

(1) Velasco, E.; Lamb, B.; Westberg, H.; Allwine, E.; Sosa, G.; Arriaga-Colina, J. L.; Jobson, B. T.; Alexander, M. L.; Prazeller, P.; Knighton, W. B.; Rogers, T. M.; Grutter, M.; Herndon, S. C.; Kolb, C. E.; Zavala, M.; de Foy, B.; Volkamer, R.; Molina, L. T.; Molina, M. J. *J. Atmos. Chem. Phys.* **2007**, *7*, 329.

(2) Offenberg, J. H.; Lewis, C. W.; Lewandowski, M.; Jaoui, M.; Kleindienst, T. E.; Edney, E. O. *Environ. Sci. Technol.* **2007**, *41*, 3972.

(3) *The Mechanisms of Atmospheric Oxidation of Aromatic Hydrocarbons*; Calvert, J. G., Atkinson, R., Becker, K. H., Kamens, R. M., Seinfeld, J. H., Wallington, T. J., Yarwood, G., Eds.; Oxford University Press: Oxford, 2002.

(4) Bloss, C.; Wagner, V.; Jenkin, M. E.; Volkamer, R.; Bloss, W. J.; Lee, J. D.; Heard, D. E.; Wirtz, K.; Martin-Reviejo, M.; Rea, G.; Wenger, J. C.; Pilling, M. J. *Atmos. Chem. Phys.* **2005**, *5*, 641.

(5) Wagner, V.; Jenkin, M. E.; Saunders, S. M.; Stanton, J.; Wirtz, K.; Pilling, M. J. *Atmos. Chem. Phys.* **2003**, *3*, 89.

(6) Birdsall, A. W.; Andreoni, J. F.; Elrod, M. J. *J. Phys. Chem. A* **2010**, *114*, 10655.

(7) Noda, J.; Volkamer, R.; Molina, M. J. *J. Phys. Chem. A* **2009**, *113*, 9658.

(8) Aschmann, S. M.; Arey, J.; Atkinson, R. *Atmos. Environ.* **2010**, *44*, 3970.

(9) Arey, J.; Obermeyer, G.; Aschmann, S. M.; Chattopadhyay, S.; Cusick, R. D.; Atkinson, R. *Environ. Sci. Technol.* **2009**, *43*, 683.

(10) Nishino, N.; Arey, J.; Atkinson, R. *J. Phys. Chem. A* **2010**, *114*, 10140.

(11) Gomez Alvarez, E.; Viidanoja, J.; Munoz, A.; Wirtz, K.; Hjorth, J. *Environ. Sci. Technol.* **2007**, *41*, 8362.

(12) NIST, Chemical Kinetics Database, http://kinetics.nist.gov/kinetics/index.jsp, accessed 3/21/11

(13) Miller, A. M.; Yeung, L. Y.; Kiep, A. C.; Elrod, M. J. *Phys. Chem. Chem. Phys.* **2004**, *6*, 3402.

(14) Seeley, J. V.; Meads, R. F.; Elrod, M. J.; Molina, M. J. *J. Phys. Chem.* **1996**, *100*, 4026.

(15) Baltaretu, C. O.; Lichtman, E. I.; Hadler, A. B.; Elrod, M. J. *J. Phys. Chem. A* **2009**, *113*, 221.

(16) Zhao, J.; Zhang, R.; Misawa, K.; Shibuya, K. *J. Photochem. Photobiol., A* **2005**, *176*, 199.

(17) Wyche, K. P.; Monks, P. S.; Ellis, A. M.; Cordell, R. L.; Parker, A. E.; Whyte, C.; Metzger, A.; Dommen, J.; Duplissy, J.; Prevot, A. S. H.; Baltensperger, U.; Rickard, A. R.; Wulfert, F. *Atmos. Chem. Phys.* **2009**, *9*, 635.

(18) Berndt, T.; Boge, O. *Phys. Chem. Chem. Phys.* **2001**, *3*, 4946.

(19) Seeley, J. V.; Jayne, J. T.; Molina, M. J. *Int. J. Chem. Kinet.* **1993**, *25*, 571.

(20) Seuwen, R.; Warneck, P. *Int. J. Chem. Kinet.* **1996**, *28*, 315.

(21) Berndt, T.; Böge, O. *Phys. Chem. Chem. Phys.* **2006**, *8*, 1205.

(22) Becker, K. H.; Barnes, I.; Bierbach, A.; Brockmann, K. J.; Kirchner, F. *Chemical Processes in Atmospheric Oxidation*; Springer-Verlag: Berlin, 1997; p 79.

(23) Jenkin, M. E.; Hayman, G. D. *J. Chem. Soc., Faraday Trans.* **1995**, *91*, 1911.

(24) Hasson, A. S.; Tyndall, G. S.; Orlando, J. J. *J. Phys. Chem. A* **2004**, *108*, 5979.

(25) Dillon, T. J.; Crowley, J. N. *Atmos. Chem. Phys.* **2008**, *8*, 4877.